

## Progress Report: Planetary Boundary Layer Height Studies with CALIOP

Award Number, NNX10AM26G: Planetary Boundary Layer Height Studies with CALIOP  
PI: Steven Ackerman

Contact Information:  
Phone: 608 263 3647  
Email: stevia@ssec.wisc.edu

### **1 Introduction**

Traditionally the horizontal and vertical structure of the planetary boundary layer (PBL) has been measured by in situ instrumentation on aircraft, towers, or balloons. Increasingly boundary layer measurements can now be made via remote sensing instrumentation such as lidar, radar, sodar, etc. With the launch of the CALIPSO satellite in 2006 many new opportunities have arose to measure boundary layer clouds and aerosols with the Cloud-Aerosol Lidar with Orthogonal Polarization (CALIOP) instrument, a two-wavelength (532 and 1064 nm) polarization sensitive lidar.

Through the PBL, exchanges of heat, moisture, momentum, and aerosol constitutes (natural and anthropogenic) occur between the free atmosphere and the surface properties (e.g. soil, vegetation, water surface). The depth of the PBL or its top height is a key parameter that determines many factors important to air quality, weather, or climate models and determines, for example, the amount of vertical diffusion and entrainment of atmospheric pollutants. In this work we present an algorithm to retrieve the convective PBL top height using CALIOP profile data and present our first large scale global results, as well as comparisons to the PBLH retrieved from Aircraft Meteorological DATA Relay (AMDAR) profile measurements of potential temperature and the NASA Langley HSRL retrievals of PBL height (PBLH).

### **2 Methodology**

During the day, with solar heating, thermal circulations create strong turbulence and cause aerosols and potential temperature to be well mixed. Air in the free-troposphere is entrained into the mixed layer, causing the mixed-layer depth to increase during the day, and forming an entrainment zone. The mixed

layer, surface layer and bottom portion of the entrainment zone are statically unstable. Aerosols trapped in the mixed layer cannot escape through the entrainment zone, the lidar being sensitive to aerosol scattering can observe the scattering contrast between the generally ‘clean’ free-atmosphere and the mixed layer. The top of the surface-aerosol layer is used as a proxy for the PBLH, a few methods have been developed to retrieve the PBLH from lidar data, and ours uses a wavelet covariance transform analysis technique similar to that found in [1]. Ours is novel in that it has been developed to work with the lower SNR data provided by CALIOP, and is intended to work autonomously, that is applied to a global data without intervention.

## 2.1 Attenuated scattering ratio and the wavelet transform method

The CALIPSO lidar CALIOP provides measurements of backscattered power, the calibrated data available in the level 1B data files is attenuated backscatter and is defined as:

$$\beta'_{Total}(z) = [\beta_m(z) + \beta_a(z)] T_m^2(z) T_{O_3}^2(z) T_a^2(z)$$

where  $\beta_m, \beta_a, T_m^2, T_a^2$ , and  $T_{O_3}^2$ , are the backscattering coefficients for molecules and aerosols, transmittances do to molecules (m), aerosols (a), and ozone (O3), respectively. Note that the aerosol term can be a stand in for any particulate scattering, i.e. aerosols or hydrometeors. Operating the wavelet transform on this profile data is inconvenient because of the molecular attenuation of the lidar signal (i.e. the  $T_m^2(z)$  term). Instead we divide the attenuated backscatter by the molecular scattering coefficient and transmittances to compute a profile of attenuated scattering ratio as:

$$f(z) = \frac{[\beta_m(z) + \beta_a(z)] T_m^2(z) T_{O_3}^2(z) T_a^2(z)}{\beta_m(z) T_m^2(z) T_{O_3}^2(z)} = \frac{[\beta_m(z) + \beta_a(z)] T_a^2(z)}{\beta_m(z)}$$

In regions where there is little or no aerosol (particulate) scattering  $f(z) = 1$ , in the PBL region where the scattering from aerosols is significant,  $f(z) > 1$ , see Figure 1 below 1.7 km in altitude.  $\beta_m$ ,  $T_m^2$ , and  $T_{O_3}^2$  are computed for each profile using the GEOS (need version) temperature, pressure, and ozone number density data that is provided in the CALIPSO lidar level 1B files.

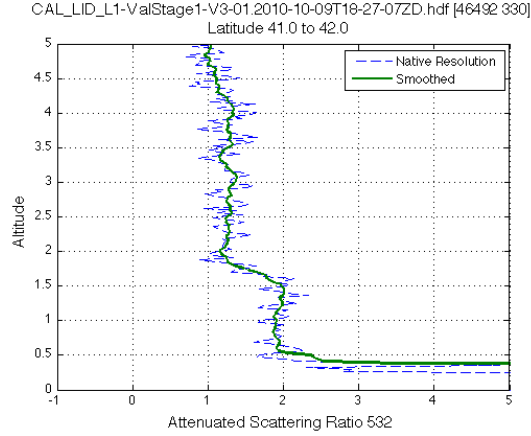


**Figure 1 Attenuated scattering ratio computed CALIPSO lidar level 1B attenuated backscatter data from 9/10/2010 near Chicago, IL.**

The wavelet covariance transform  $W_f(a, b)$  is computed for each lidar profile  $f(z)$ , as the following:

$$W_f(a, b) = \frac{1}{a} \int_{z_b}^{z_t} f(z) h\left(\frac{z-b}{a}\right) dz$$

where  $z_b$ , and  $z_t$  are the bottom and top of the lidar measurement profile, and  $h$  is the Haar function:

$$h\left(\frac{z-b}{a}\right) = \begin{cases} +1: & b - \frac{a}{2} \leq z \leq b \\ -1: & b \leq z \leq b + \frac{a}{2} \\ 0: & \text{elsewhere,} \end{cases}$$

where  $z$  is the altitude,  $b$  is the translation, and  $a$  is the dilation. Before the wavelet covariance transform is calculated it is critical that we mask out the lidar surface return signal, if left in the lidar signal it will completely overwhelm the transform signal, making the PBLH retrieval extremely difficult or impossible. Currently the covariance transform is computed over a range of dilations from 0.9 to 1.65 km in 30 m steps, and a mean value profile is generated across the range of dilation values as,  $\overline{W_f(b)} =$

$\frac{1}{n} \sum_{i=1}^n W_f(a_i, b)$ . The profile of  $\overline{W_f(b)}$  is then searched for local minima from the surface upward. From our case studies we have found that this method is superior to that used in [1] for the lower SNR CALIPSO data, as  $\overline{W_f(b)}$  is more likely to present one unique minima at the correct altitude.

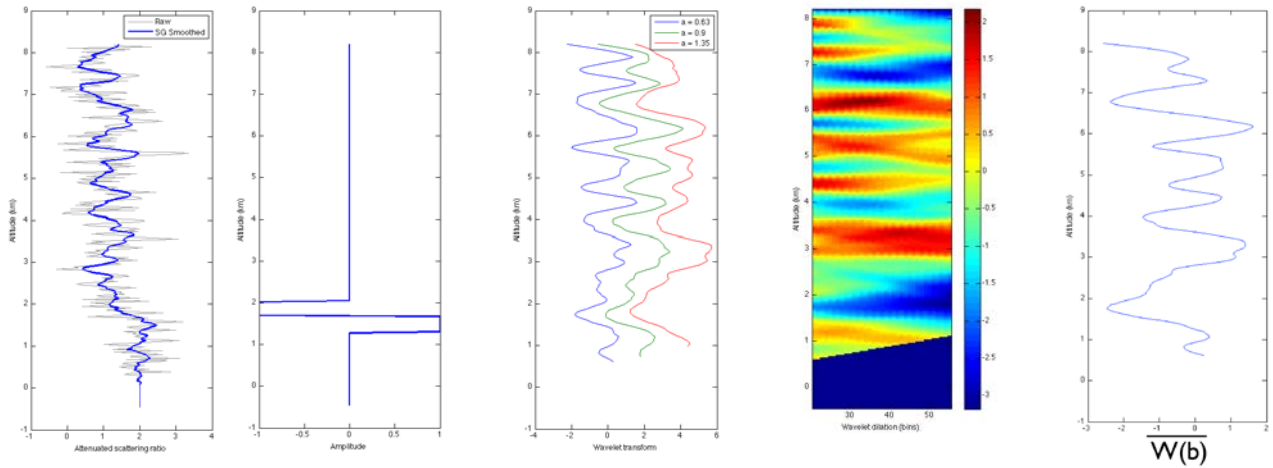


**Figure 2** Graphical representation of the workflow from attenuated scattering ratio (left) to computing the mean wavelet transform (right).

## 2.2 AMDAR retrievals

The validation strategy for this study involves comparisons of PBL height from Aircraft Meteorological Data Relay (AMDAR) commercial aircraft observations of temperature, water vapor, and pressure. Given that potential temperature is nearly constant in the convective boundary layer, by finding the inflection point we can estimate the PBL height from these AMDAR measurements. AMDAR data from Chicago O’ Hare, Atlanta Hartsfield Jackson, Honolulu, and Las Vegas McCarran International Airports were selected for comparison against CALIOP for 18 UTC.

PBLH estimates for AMDAR data were determined following the Liu and Liang’s (2009) automated PBLH detection procedure. This method first classifies the boundary layer as stable, unstable or neutral, based on examination of the potential temperature ( $\theta$ ) profile. Boundary layer height is then determined by an objective algorithm based on the theoretical  $\theta$  profile of each regime. However, application of this method requires a full vertical  $\theta$  profile, which includes surface-level potential

temperature data, which is not available in AMDAR observations. Therefore, NCDC hourly surface observations were appended to the AMDAR potential temperature profile to obtain the full theta profile.

Once a more complete theta profile was assembled, the AMDAR data was re-gridded using linear interpolation. The height intervals selected for re-gridding range from 25m to 600m. The table below shows the height intervals that were employed for re-gridding of the AMDAR data are:

**Table 1 Height intervals that were employed for re-gridding of the AMDAR data**

| Range       | Interval |
|-------------|----------|
| 0m-600m     | 25m      |
| 600m-800m   | 50m      |
| 800m-1400m  | 100m     |
| 1400m-2300m | 150m     |
| 2300m-3100m | 200m     |
| 3100m-3600m | 500m     |
| 3600m-4200m | 600m     |

Once the data was re-gridded, the Liu and Liang PBLH determination algorithm was applied to AMDAR data to obtain PBL height estimates. Details on the procedure for PBLH determination can be found in Liu and Lang (2009). A brief overview of the algorithm will be given i for completeness.

The automated PBLH detection procedure developed by Liu and Liang involves two main steps: 1. Classify the boundary layer into a stable (SBL), unstable (CBL), or neutral (NRL) regime 2. Determine PBLH based on the theoretical theta profile. To classify the boundary layer into a regime, the algorithm examines the near-surface thermal gradient between the second and fifth levels using the criteria shown below:

$$\theta_5 - \theta_2 \begin{cases} < -\delta_s & \text{for CBL} \rightarrow \text{an unstable regime} \\ > +\delta_s & \text{for SBL} \rightarrow \text{a stable regime} \\ \text{else} & \text{for NRL} \rightarrow \text{a neutral regime} \end{cases} ,$$

where  $\theta$  is potential temperature (Kelvin), and  $\delta_s$  is the  $\theta$  increment for the minimum strength of the stable layer above the CBL top or below the SBL top. The subscript below the  $\theta$  symbol denotes the data level index. The second level is selected for this test to avoid surface noise. The values of  $\delta_s$  to be employed will depend on surface characteristics. Liu and Liang (2009) determined values for  $\delta_s$  through visual validation with trial and error for ice, ocean, and land. For the purpose of this study, a  $\delta_s$  of 1.0K was selected as the data was collected over land.

Once the boundary layer is classified into a certain regime, a numerical procedure is employed to determine boundary layer height for each regime. For the convective case, Stull (1988) defines the PBLH as the height at which the air parcel becomes neutrally buoyant. Therefore, an upward scan of the  $\theta$  profile is performed to find the lowest level  $l=k$  that satisfies:

$$\theta_k - \theta_1 \geq \delta_u,$$

where  $\delta_u$  is the  $\theta$  increment for the minimum strength of the unstable layer, which in this case is .5K (from Liu and Liang 2009). Then, a second scan is pursued to correct for the first scan to find the first occurrence of:

$$\dot{\theta}_k \equiv \frac{\partial \theta_k}{\partial z} \geq \dot{\theta}_r,$$

where  $\dot{\theta}_r$  is the  $\theta$  vertical gradient per height  $z$  and  $\dot{\theta}_r$  is its minimum strength for the overlying inversion layer, which is 4.0K/km (Liu and Liang, 2009).  $\dot{\theta}_r$  will be defined as the boundary layer top. The same procedure is employed to determine the PBLH for the neutral case.

For the stable case, the PBLH is difficult to estimate without actual measurements of the turbulent kinetic energy profile in the boundary layer (Stull 1988; Seibert et al. 2000). The procedure employed to determine the PBLH for the stable case will depend on whether the SBL turbulence is a result of buoyancy forcing or shear. The boundary layer is first tested to determine if the turbulence is buoyancy forced. If it does not satisfy the criteria for buoyancy forcing, the methodology to determine PBLH for the shear driven case is employed.

To determine if the SBL is forced by buoyancy, an upward scan of the theta profile is performed to find the lowest level at which  $\dot{\theta}_r$  reaches a minimum. The PBLH will be determined at that height if the conditions below are satisfied:

$$\begin{cases} \dot{\theta}_k - \dot{\theta}_{k-1} < -\delta & \text{or} \\ \dot{\theta}_{k+1} < \dot{\theta}_r, \quad \dot{\theta}_{k+2} < \dot{\theta}_r, \end{cases}$$

where the first condition ensures that  $\theta_k$  is a local peak with a curvature parameter  $\delta_r$  of  $40 \text{ K km}^{-1}$  while the second condition constrains that an inversion layer is not evident in the upper two layers. The determined PBLH will represent the transition from the stable layer to a neutral or unstable condition above (Liu and Liang, 2009).

Results of this automated processing is shown in Figure 1 (right side), potential temperature vs altitude plots (below). The aircraft data within +/- 1 hour of the CALIPSO overpass closest to the airport are collected and a potential temperature profile generated, outlying points are screened using a Grubbs test. We then use the algorithm in [2] to determine the top of PBL from the potential temperature profile.

### 2.3 HSRL LaRC

The airborne HSRL developed by NASA Langley (LaRC) (Hair et. al. 2008) has been deployed to over ten field experiments, logging nearly 800h on 240 flights of the LaRC King Air B-200 aircraft. Many of these flights were flown expressly along the CALIPSO ground track to aid in the validation of CALIPSO data products (see Rogers 2011 for complete list of coincident flights). The HSRL technique allows the aerosol backscatter and extinction to be measure independently at 532 nm. Additionally the HSRL measure polarization state at 532 nm, 1064 nm, and backscatter at 1064 nm. Data products are produced with no assumptions in the calibration and with few assumptions in the aerosol retrieval algorithms. The HSRL team has also implemented a PBLH retrieval scheme using a wavelet technique similar to what is found in (Brooks, 2003). These qualities make the HSRL the ideal platform with which to evaluate the CALIOP PBLH retrievals.

## 3 Validation

### 3.1 CALIOP vs AMDAR

Here are shown results from one case study of our automated retrievals from both the lidar wavelet transform and the AMDAR potential temperature retrieval (Figure 3) the yellow and orange colors of the attenuated backscatter image indicate the enhanced scattering from aerosols in the mixed layer. For the majority of the profiles the lidar retrieval performs well, however it is clear in 3 instances (i.e. near 33.6, 34, and 36 latitude) the retrieval is extremely low; the mean PBLH over this range latitude range is ~2500 m. The automated AMDAR retrieval also performs quite well in this instance as it is clear that there is a strong inversion located at 2845 m, note that there is a weaker inversion near 2000 m. As only one aircraft sample was available for this case and CALIPSO closest approach was nearly 80 km west of Hartsfield airport, this comparison is encouraging. Similar case studies from both Atlanta and Chicago provide similar or better agreement.

For the period June 2006 through April 2012 we compiled set of coincident PBLH retrievals at Chicago, Il airport (ORD) with the criteria that the aircraft AMDAR observations had to be made within +/- 1 hour of the CALIPSO overpass, and the CALIPSO ground track must have passed within 100 km (abeam) of ORD (Figure 4).

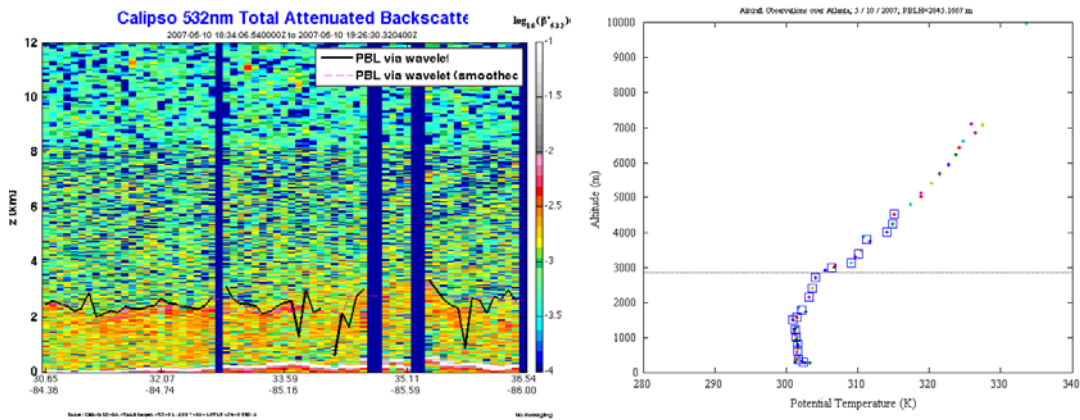


**Figure 3 (Left) CALIPSO total attenuated backscatter image near Atlanta (ATL), 2007-05-10, black line indicates PBLH wavelet transform, blue bars are missing data due to cloud clearing. (Right) AMDAR potential temperature profile +/- 1 hour of CALIPSO overpass hour.**



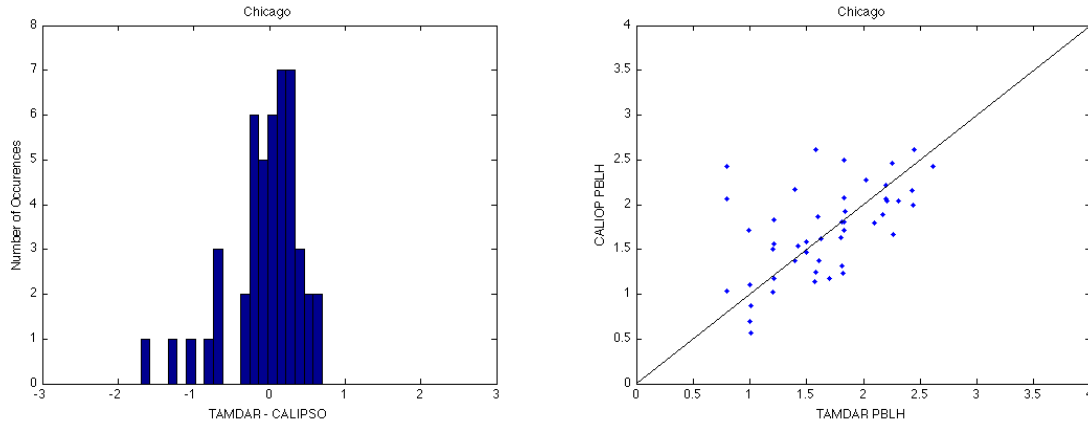


**Figure 4 Comparison of coincident TAMDAR – CALIPSO retrievals at Chicago, IL, USA, (ORD) for the period June, 2006, April 2012, 47 coincidences in total.**

### 3.2 CALIOP vs LaRC HSRL

Coincident retrievals of the PBLH from CALIOP and the NASA LaRC airborne HSRL instrument during TEXAQS are shown in Figure 5.

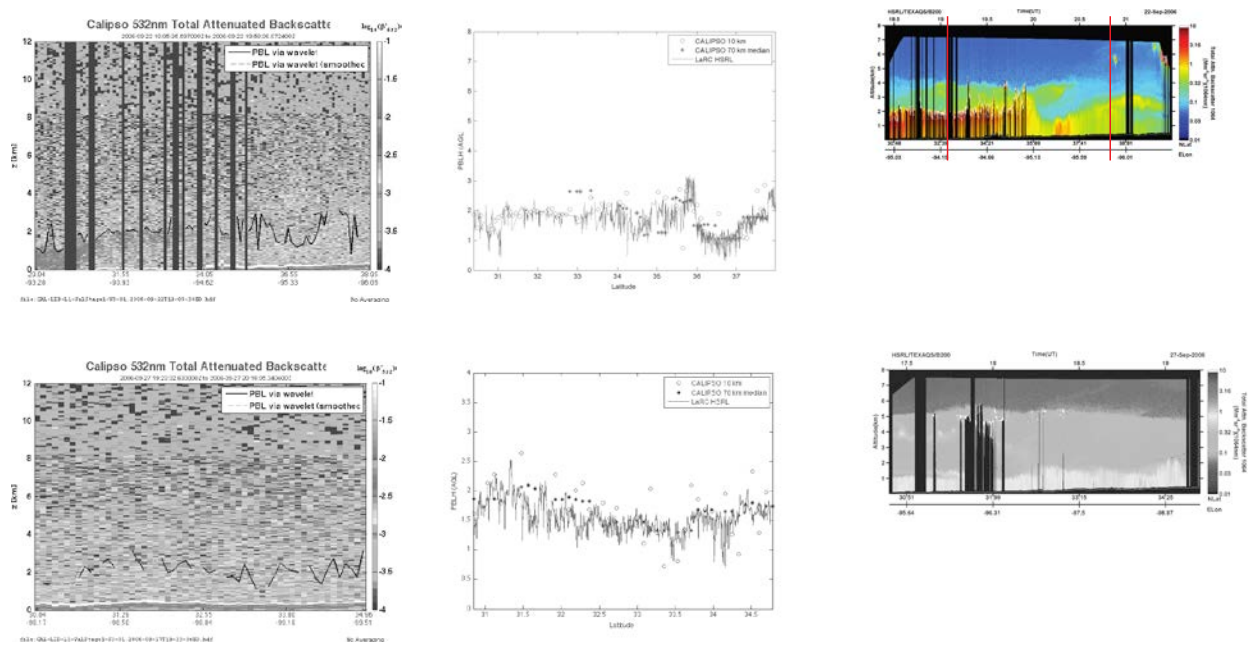


**Figure 5 Profiles of CALIOP attenuated backscatter (left), PBLH retrievals (center), and LaRC HSRL attenuated backscatter are show for 9/22/2006 (top row) and 9/27/2006 (bottom row) for the TEXAQS experiment.**

## 4 Applications

We have the run the algorithm on 6 years of CALIPSO lidar data from June 2006, to November 2012 the results are shown in Figure 6 with the number of retrieval in Figure 7. There global results are reasonable, for example the boundary layer is higher over the deserts in summer than in the winter, though the PBLH of some deserts seems a bit low in altitude. The retrieved PBLH are reasonable over the oceans, being generally less than 2 km.

Our next plan is to submit a paper on this and make the data publically available.

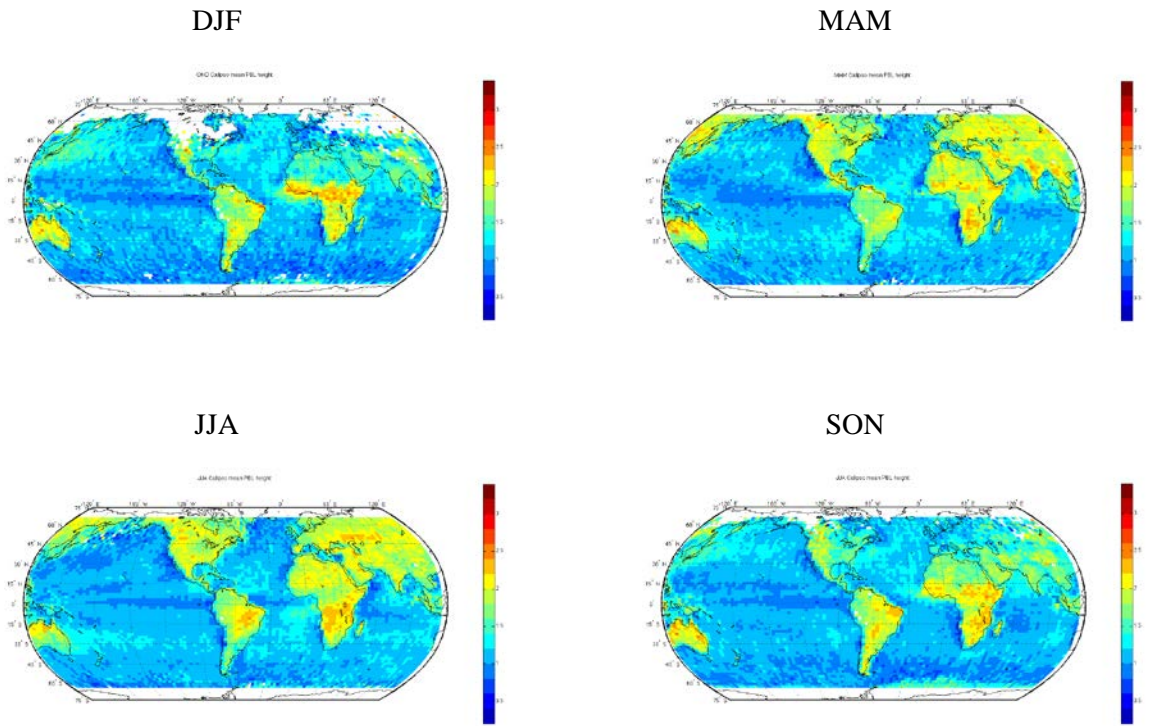


**Figure 6 Global mean PBL height (above ground level) for 6 years (June 2006, November 2012), 2x3 degree grid boxes.**

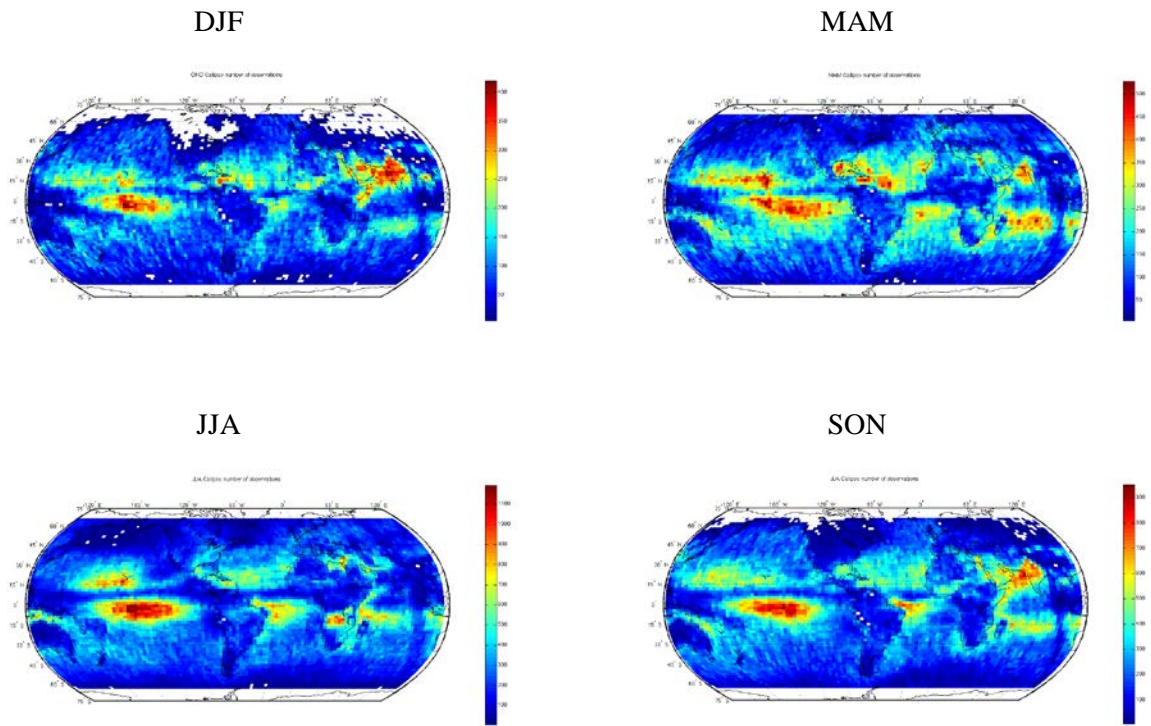


Figure 7 Number of PBLH retrievals per grid box for 6 years (June 2006, November 2012), 2x3 degree grid boxes.

## 5 Summary

We have shown a method to retrieval the PBL top height from space-borne lidar data for the daytime convective boundary layer. In addition we have started a validation program using AMDAR measurements of potential temperature and comparing the retrieved PBLH. In the near future the data will be staged on our data server for access by interested scientists.

## 6 References

- [1] K.J. Davis, N. Gamage, C.R. Hagelberg, C. Kiemle, D.H. Lenschow and P.P. Sullivan, "An Objective Method for Deriving Atmospheric Structure from Airborne Lidar Observations," *J. Atmos. Sci.*, AMS, 17, pp. 1455-1468, November 2000.
- [2] S. Liu and X.Z. Liang, "Observed Diurnal Cycle Climatology of Planetary Boundary Layer Height," *J. of Climate*, AMS, 23, pp. 5790-5809, November 2010.
- [3] Hair, J. W., Hostetler, C. A., Cook, A. L., Harper, D. B., Ferrare, R. A., Mack, T. L., Welch, W., Isquierdo, L. R., and Hovis, F. E.: Airborne High Spectral Resolution Lidar for Profiling Aerosol Optical Properties, *Appl. Optics*, 47(36), 6734–6752, doi:10.1364/AO.47.006734, 2008.
- [4] Rogers, R. R., C. A. Hostetler, J. W. Hair, R. A. Ferrare, Z. Liu, M. D. Obland, D. B. Harper, A. L. Cook, K. A. Powell, M. A. Vaughan, and D. M. Winker: Assessment of the CALIPSO Lidar 532 nm attenuated backscatter calibration using the NASA LaRC airborne High Spectral Resolution Lidar, *Atmos. Chem. Phys.*, 11, 1295–1311, 2011
- [5] Brooks, I. M.: Finding Boundary Layer Top: Application of a Wavelet Covariance Transform to Lidar Backscatter Profiles, *J. Atmos. Ocean Tech.*, 20, 1092-1105, 2003